Supplementary Material for "Constraining the geothermal heat flux in Greenland at regions of radar-detected basal water"

Soroush Rezvanbehbahani*[1,2], Leigh A. Stearns[1,2],
C.J. van der Veen[3], Gordon K.A. Oswald[4], and Ralf Greve[5]

[1]Department of Geology, University of Kansas, Lawrence, KS 66045, USA
[2]Center for Remote Sensing of Ice Sheets, University of Kansas, Lawrence, KS 66045, USA
[3]Department of Geography and Atmospheric Science, University of Kansas, Lawrence, KS 66045, USA
[4]Climate Change Institute, University of Maine, Orono, ME 04469, USA
[5]Institute of Low Temperature Science, Hokkaido University, Sapporo, Japan

S1 GHF constraints at OSW thawed points

Figure S1 shows the estimated GHF_{pmp} values at the thawed-bed predictions by OSW data. In every row, the left panel shows the calculated GHF_{pmp}; the middle and right panels show the concomitant offset of initial and final surface elevation and surface velocity maps, respectively. For the majority of the ice sheet, the initial surface elevation and velocity maps have been preserved, confirming that the present-day ice sheet is reproduced. The melting point criteria (i.e. $T_b > -0.1°\mathrm{C}$ relative to the pressure melting point or $\dot{M}_b < 0.001$ m yr^{-1}) are satisfied for all simulations with the OSW dataset.

S2 GHF constraints at JOR thawed points

The estimated GHF_{pmp} at the locations of JOR dataset and different initial GHF models are shown in Fig. S2.

S3 Constraints on basal melt rate $\dot{M}_b$

Comparison between the values of total basal melt rate before and after GHF adjustments for each GHF map for both OSW and JOR data is shown in Table S1.

*soroushr@ku.edu

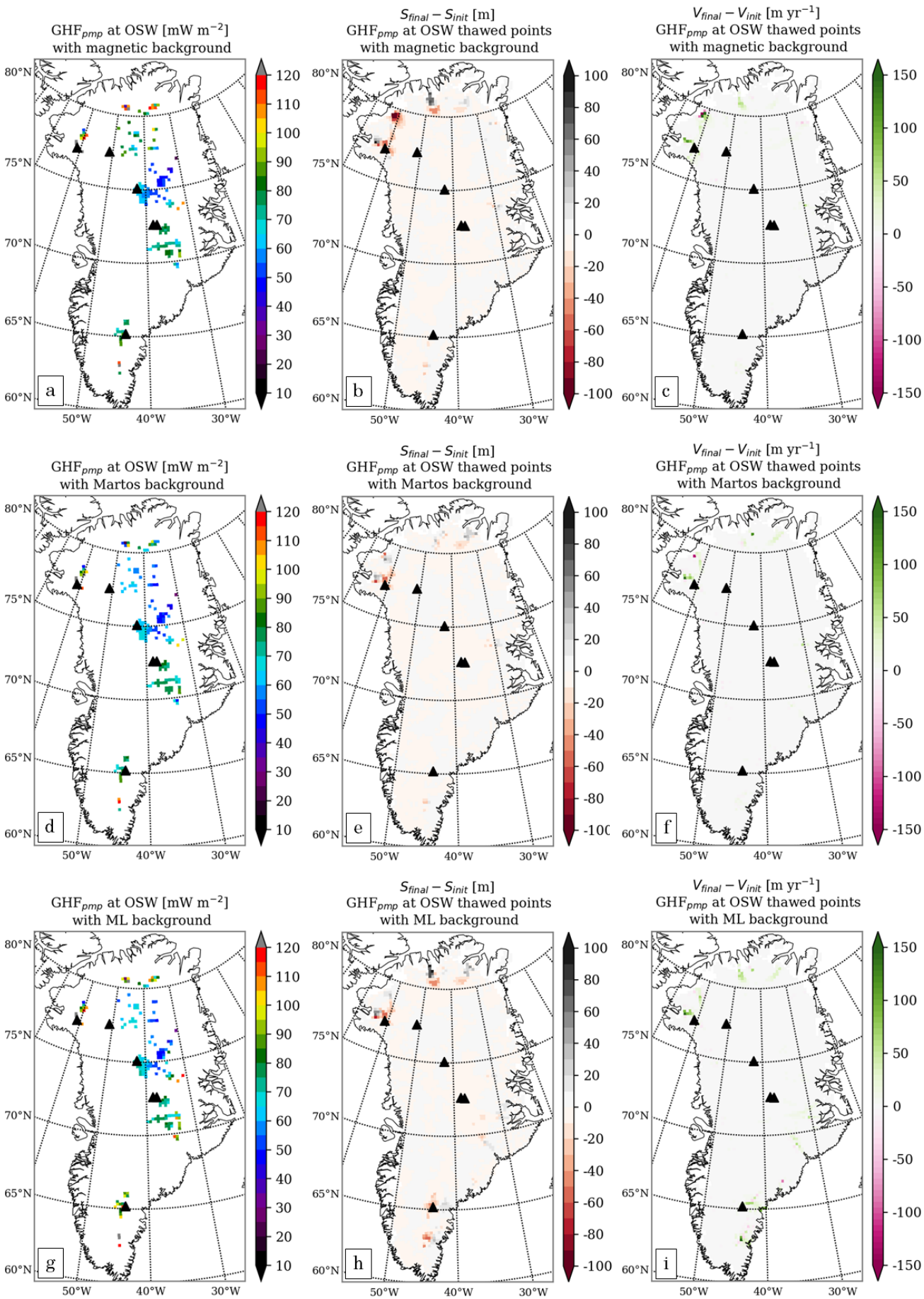
GHF$_{pmp}$ at OSW [mW m^{-2}]
with magnetic background
$S_{final} - S_{init}$ [m]
GHF$_{pmp}$ at OSW thawed points
with magnetic background
$V_{final} - V_{init}$ [m yr^{-1}]
GHF$_{pmp}$ at OSW thawed points
with magnetic background
GHF$_{pmp}$ at OSW [mW m^{-2}]
with Martos background
$S_{final} - S_{init}$ [m]
GHF$_{pmp}$ at OSW thawed points
with Martos background
$V_{final} - V_{init}$ [m yr^{-1}]
GHF$_{pmp}$ at OSW thawed points
with Martos background
GHF$_{pmp}$ at OSW [mW m^{-2}]
with ML background
$S_{final} - S_{init}$ [m]
GHF$_{pmp}$ at OSW thawed points
with ML background
$V_{final} - V_{init}$ [m yr^{-1}]
GHF$_{pmp}$ at OSW thawed points
with ML background
80°N
75°N
70°N
65°N
60°N
50°W
40°W
30°W
a
b
c
d
e
f
g
h
i

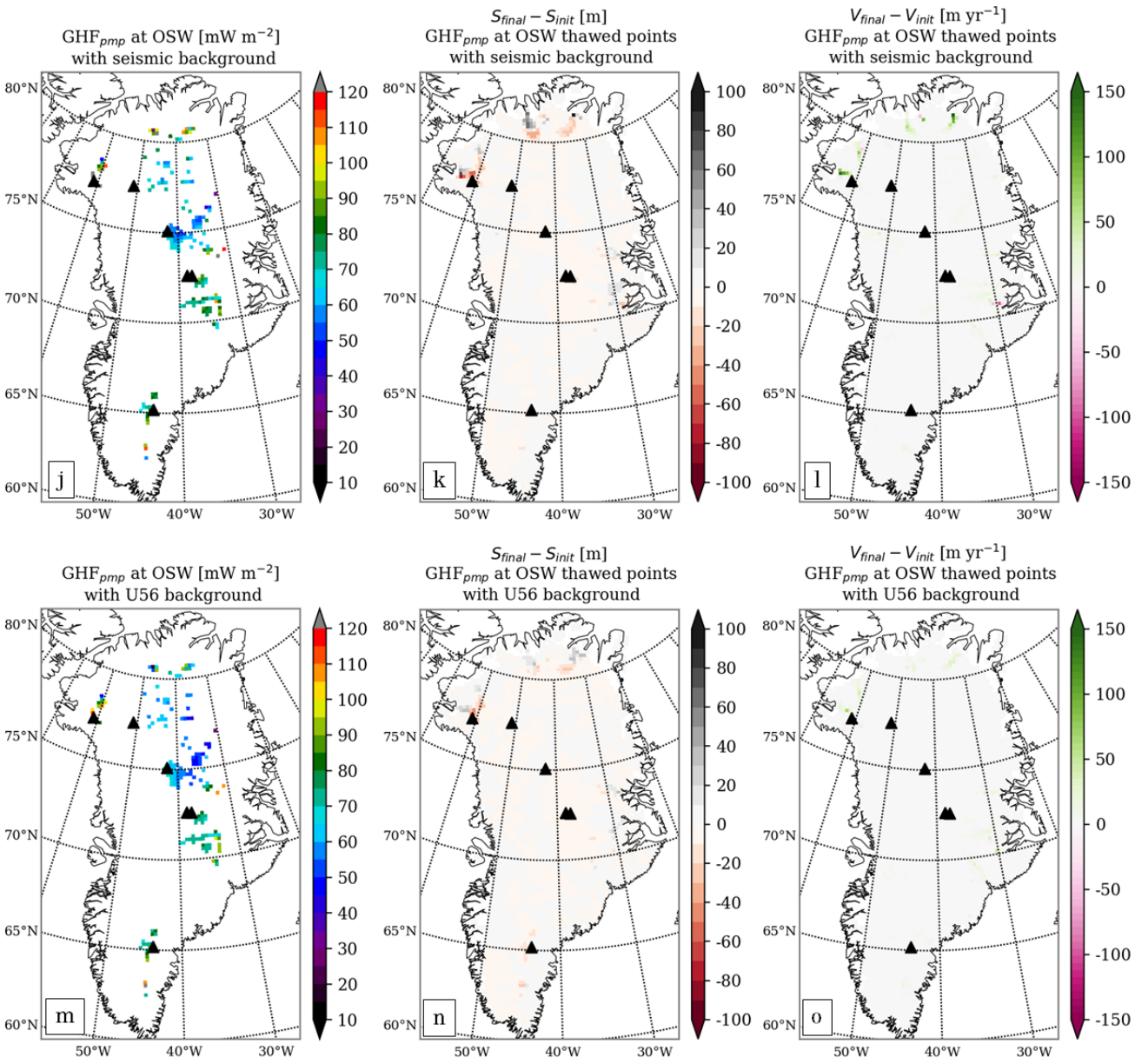

Figure S1: Estimated GHF$_{pmp}$ at locations of basal thaw provided by Oswald and others (2018) using five different GHF maps and the resultant elevation and surface velocity offset after GHF iterations with respect to the initial geometry. Each row shows the GHF$_{pmp}$ with a different 'background' GHF map; (a-c) Fox Maule and others (2009), (d-f) Martos and others (2018), (g-i) Rezvanbehbahani and others (2017), (j-l) Shapiro and Ritzwoller (2004), and (m-o) uniform GHF of 56 mW m^{-2}.

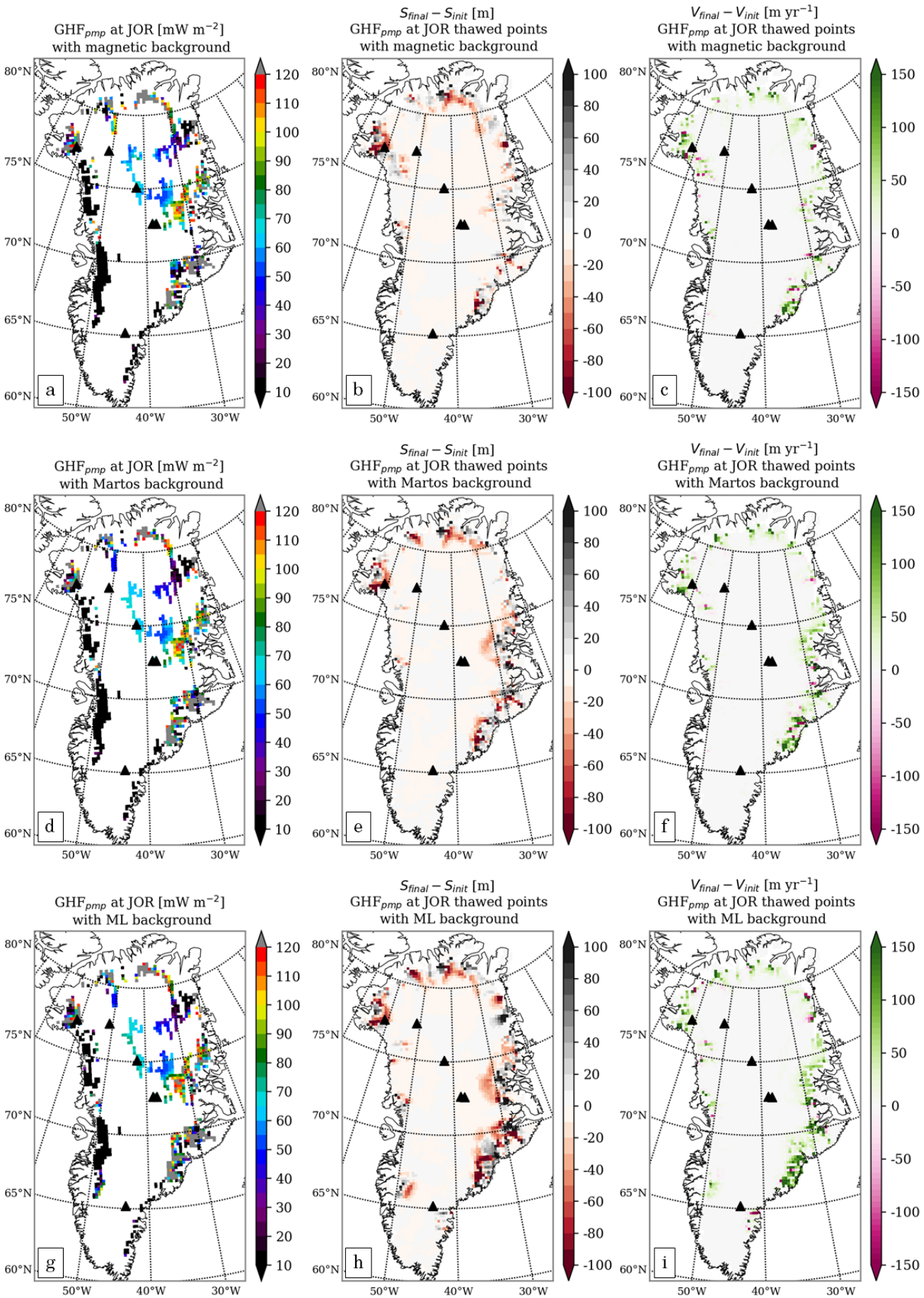
GHF$_{pmp}$ at JOR [mW m^{-2}]
with magnetic background
$S_{final} - S_{init}$ [m]
GHF$_{pmp}$ at JOR thawed points
with magnetic background
$V_{final} - V_{init}$ [m yr^{-1}]
GHF$_{pmp}$ at JOR thawed points
with magnetic background
GHF$_{pmp}$ at JOR [mW m^{-2}]
with Martos background
$S_{final} - S_{init}$ [m]
GHF$_{pmp}$ at JOR thawed points
with Martos background
$V_{final} - V_{init}$ [m yr^{-1}]
GHF$_{pmp}$ at JOR thawed points
with Martos background
GHF$_{pmp}$ at JOR [mW m^{-2}]
with ML background
$S_{final} - S_{init}$ [m]
GHF$_{pmp}$ at JOR thawed points
with ML background
$V_{final} - V_{init}$ [m yr^{-1}]
GHF$_{pmp}$ at JOR thawed points
with ML background
80°N
75°N
70°N
65°N
60°N
50°W
40°W
30°W
a
b
c
d
e
f
g
h
i
120
110
100
90
80
70
60
50
40
30
20
10
100
80
60
40
20
0
-20
-40
-60
-80
-100
150
100
50
0
-50
-100
-150

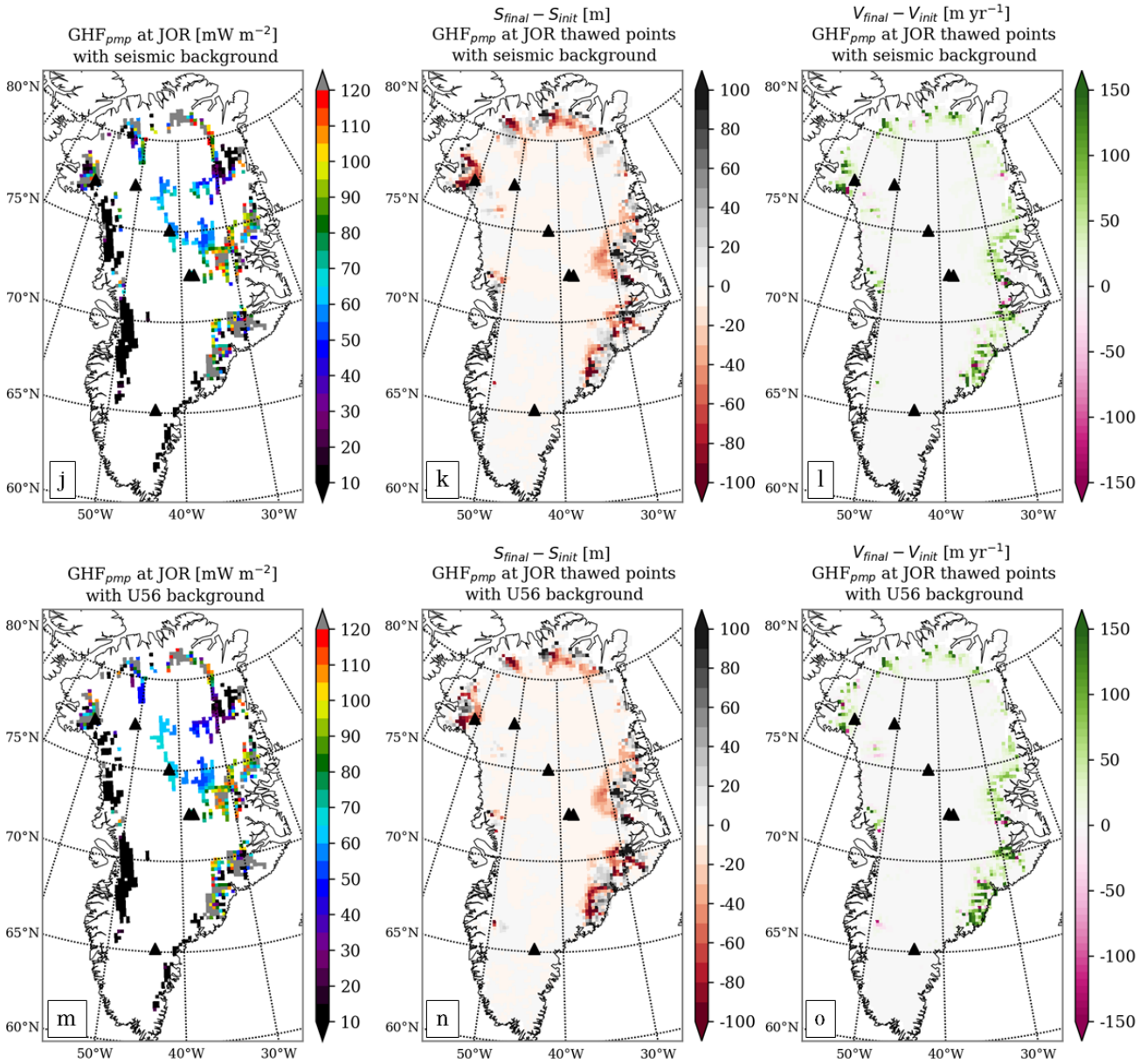

Figure S2: Same as Fig. S1, with GHF adjustments at the locations of basal water detected by Jordan and others (2018).

Table S1: Basal melt rate [$km^3\ yr^{-1}$] for individual catchments of the GrIS. Three sets of basal melt rates are reported (first column). First the basal melt rate for each catchment using all GHF maps prior to any adjustment at locations of thawed bed. Second, the basal melt rates for all catchments with all GHF maps are reported after modifying the GHF at OSW thawed locations, and the third set of simulations are after modifying the GHF at JOR thawed points. The modified heat flux is defined as GHF_{mod}=max(GHF, GHF_{pmp}). Catchment boundaries are chosen similar to Csathó and others (2014), and $\Sigma\dot{M}_b$ is the sum of basal melt rate in all catchments.

Simulation	GHF	Central-West	Central-East	North	Northeast	Northwest	Southeast	Southwest	$\Sigma\dot{M}_b$
GHF before adjustment	magnetic	2.16	1.14	0.84	0.37	3.00	7.27	2.85	17.65
	Martos	2.38	0.70	0.91	0.78	3.69	6.86	2.76	18.09
	ML	2.15	0.33	0.9	0.85	3.57	5.09	1.38	14.27
	seismic	2.09	0.47	0.54	0.34	3.12	7.12	2.87	16.46
	U56	2.29	0.43	0.85	0.66	3.79	6.38	2.45	16.85
GHF_{mod} at OSW	magnetic	2.17	1.09	0.88	0.35	2.96	7.26	2.87	17.60
	Martos	2.39	0.89	1.02	0.85	3.86	7.31	2.76	19.10
	ML	2.16	0.37	0.97	0.87	3.61	5.29	1.37	14.65
	seismic	2.10	0.50	0.60	0.40	3.18	7.14	2.87	16.81
	U56	2.30	0.46	0.89	0.68	3.82	6.44	2.46	17.06
GHF_{mod} at JOR	magnetic	2.18	1.22	0.96	0.50	3.30	7.57	2.87	18.62
	Martos	2.39	0.90	1.02	0.86	3.86	7.31	2.76	19.10
	ML	2.16	0.62	1.04	3.68	3.78	5.82	1.44	18.56
	seismic	2.11	0.71	0.72	0.49	3.40	7.55	2.87	17.87
	U56	2.30	0.69	0.96	0.75	3.96	7.00	2.45	18.13

References

Csathó, BM, AF Schenk, C J van der Veen, G Babonis, K Duncan, S Rezvanbehbahani, MR van den Broeke, SB Simonsen, S Nagarajan and JH van Angelen, 2014. Laser altimetry reveals complex pattern of Greenland Ice Sheet dynamics, *Proceedings of the National Academy of Sciences*, **111**(52), 18478–18483.

Fox Maule, C, M E Purucker and N Olsen, 2009. Inferring magnetic crustal thickness and geothermal heat flux from crustal magnetic field models, *Danish Climate Centre Report*, 09–09.

Jordan, T M, C N Williams, D M Schroeder, Y M Martos, M A Cooper, M J Siegert, J D Paden, P Huybrechts and J L Bamber, 2018. A constraint upon the basal water distribution and thermal state of the Greenland Ice Sheet from radar bed echoes, *The Cryosphere*, **12**(9), 2831–2854.

Martos, Yasmina M., Tom A. Jordan, Manuel Cataln, Thomas M. Jordan, Jonathan L. Bamber and David G. Vaughan, 2018. Geothermal Heat Flux Reveals the Iceland Hotspot Track Underneath Greenland, *Geophysical Research Letters*, **45**(16), 8214–8222.

Oswald, Gordon KA, Soroush Rezvanbehbahani and Leigh A Stearns, 2018. Radar evidence of ponded subglacial water in Greenland, *Journal of Glaciology*, **64**(247), 711–729.

Rezvanbehbahani, Soroush, Leigh A. Stearns, Amir Kadivar, J. Doug Walker and C. J. van der Veen, 2017. Predicting the Geothermal Heat Flux in Greenland: A Machine Learning Approach, *Geophysical Research Letters*, **44**(24), 12,271–12,279.

Shapiro, N M and M H Ritzwoller, 2004. Inferring surface heat flux distributions guided by a global seismic model: particular application to Antarctica, *Earth and Planetary Science Letters*, **223**(1), 213–224.